Geometry Information-based Practical Device Identification for Local Device-to-device Communication

Eun-hye Park*, Kwang-Eog Lee**, Joon-hyuk Kang*

Abstract Local device-to-device (D2D) communication between two smart mobile devices is becoming increasingly popular. The first key step in starting a D2D communication is to discover and identify the remote target device to establish a link. However, existing device discovery mechanisms either require users to explicitly identify the ID of the target device or rely on inaccurate beamforming technology. This paper presents two novel device identification algorithms using a variety of embedded sensors. The algorithms only require that users to point two devices towards each other. This paper describes the algorithms, analyzes their accuracy using analytical models, and verifies the results using simulations.

Key Words : Augmented reality, Device identification, D2D communication, User interface

1. Introduction

Mobile traffic has been rapidly growing due to the popularization of smart phones and tablets which consume large amount of multimedia content [1]. This places a huge burden on the mobile infrastructure because most of the traffic passes through the base station. Local D2D communication provides a promising alternative to reduce this burden by allowing two neighboring devices to directly transmit and receive data using WiFi or Blutooth [2].

In a local D2D communication, a pair of devices that want to talk to each other is within proximity. The first key step is to identify the other device to establishment a communication link. However, this procedure is often very cumbersome and not user-friendly. In most cases, a user has recognized what the communication target device (TD) is, but not for its identification (ID). Similar to the WiFi access point association procedure, most techniques are list-based manual device selection, where users have to know the other device's ID or name to choose the device from a candidate list [3]. To address the shortcomings, Kwak et al. [4] proposed a beamforming based ''point-and-link'' technique for device identification. In this approach, the user points her device to the target and using beamforming the device directs its signal towards the target device to initiate the D2D communication. However, not all devices support beamforming, and beam configurations are difficult to calibrate as they are device-specific in nature [5].

In this paper, we introduce two novel solutions for device identification using

* Corresponding Author : Department of Electrical Engineering Professor of Joonhyuk Kang (jhkang@ee.kaist.ac.kr)
** Corresponding Author : Doctor of Agency for Defense Development
Received : November 04, 2014 Revised : November 18. 2014 Accepted : December 1. 2014

geometry information estimated by existing sensors, such as camera, magnetometer, GPS, or multiple antennas of wireless devices. In particular, we investigate a GPS-based device identification technique and an angle-of-arrival (AoA) based scheme. In both schemes, we ask the user to point towards the TD and align the center of the viewfinder with the TD as shown in Fig. 1. In the GPS-based scheme, a communication initiating device, or a user's device (UD) gathers the GPS information of all nearby candidate devices and identifies the TD which is at the center of UD's viewfinder. Here, note that the angular information of TD is required to know UD's direction. In this paper, we assume UD has a magnetometer function.

We further analyze its accuracy with respect to sensor errors. In the AoA-based technique, the UD estimates the angles of incident signals from all the candidate devices and identifies the TD based on the AoA. We provide an accuracy analysis for the proposed scheme by using Cramer-Rao (CR) variance and MUSIC estimator variance [6]. The main contributions of this work are listed as follows:

- We propose two user-friendly device identification techniques for D2D communication based on the geometry information that have an intuitive user interface.

- We derive the probability of misidentification using analysis and computer simulations for both techniques. We demonstrate their effectiveness of with respect to various parameters, such as sensor errors, number of antennas, and the signal-to-noise ratio (SNR).

Finally, we believe that our schemes can easily be applied to other location-based services because they are based on geometric information.

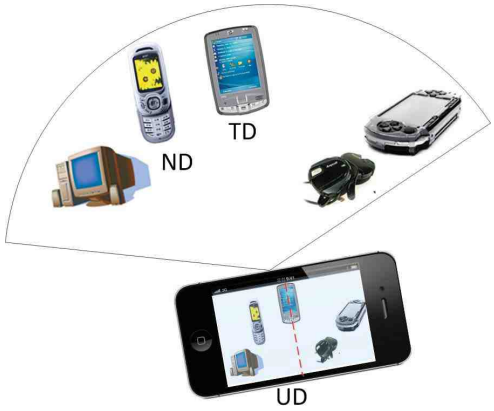

[Fig. 1] Device identification in device-to-device communications

The rest of this paper is organized as follows. In section 2, we describe two proposed device identification schemes for local D2D communication and their performance analysis in detail. Section 3 presents simulation results for both schemes and identifies the necessary conditions to achieve the required accuracy. Finally, we conclude in section 4.

2. Geometry Information-based Device Identification

2.1 System overview

Fig.1 shows how our device identification mechanism would work in practice. We assume that TD whose ID is unknown, is in the visible range from the UD (i.e., line-of-sight). The system then activates the camera and displays the obtained image in real time. Finally, it asks the user to align the TD to the center line of the viewfinder.

Our algorithms automatically identify the TD using geometric information. The

location-based algorithm can be applied when all devices have their GPS information and the UD is equipped with a magnetometer. Based on the location of each device and the user's orientation, the UD identifies the target. The AoA-based algorithm is an alternative scheme that can be used when the location information is not available. It estimates the incident angle of the signal from all candidate devices using subspace-based super-resolution algorithms such as multiple signal classification (MUSIC), ESPRIT, or MP [6],[7]. Our algorithm then identifies the TD using the AoA information. We analyze and evaluate the performance of MUSIC in this paper. Note that we consider two dimensional space, assuming all the devices are located in the same altitude.

2.2 GPS-based device ddentification

1) The UD broadcasts a request signal to its neighboring devices (NDs)
2) NDs respond to the request by sending their GPS coordinates and IDs using collision avoidance schemes such as carrier sense multiple access. We denote the coordinate of a device D, by (x_D, y_D), where x_D and y_D are the latitude and longitude of the device D, respectively.
3) The UD calculates the angles of TD and ND relative to the UD, which are defined as

$$\theta_D = \arctan\left(\frac{y_D - y_{UD}}{x_D - x_{UD}}\right) \quad (1)$$

4) UD estimates the heading angle γ of itself using its magnetometer.
5) UD now selects the device that is the closest to the heading angle γ as TD.

We now analyze the accuracy of the algorithm in the face of errors. In practice, there are two sources of errors: a GPS error and a magnetometer error. In the case of GPS, because the devices are within the visible range (0m to 70m) and we take of offset between two locations, we expect the error to be negligible. This is similar to the concept of differential GPS (DGPS), whose accuracy is known to degrade by 0.67m for each 100km distance [8]. Thus, we assume θ_{TD} and θ_{ND} do not contain any error term in third step. However, the magnetometer error can occur in the fourth step due to several factors. For instance, changes in earth magnetic field, and the existence of other electric devices can affect a magnetometer. Therefore, the modified fourth step with an error term should be written as $\hat{\gamma} = \gamma + t$,, where $\hat{\gamma}$ is the estimated heading angle, and t is the magnetometer error term. Considering a number of factors, such as electric devices nearby and the change of geomagnetism, we assume that t is a Tikhonov random variable with zero-mean and variance of σ_θ^2 [9] without loss of generality.

To analyze the misidentification probability, let $\Delta\theta$ be a difference between the angles of θ_{TD} and θ_{ND}. Mismatching occurs when an error term is greater than $\Delta\theta/2$. The mismatching probability can be obtained as

$$\begin{aligned} P_e &= P\left[t \geq \frac{\Delta\theta}{2}\right] \quad (2) \\ &= 1 - F_T\left(\frac{|\theta_{ND} - \theta_{TD}|}{2\sigma_\theta}\middle| 0, \sigma_\theta^2\right), \end{aligned}$$

where $F_T(x|\mu, \sigma_\theta^2)$ is the cumulative density

function (CDF) of the random variable t with mean μ and variance σ_θ^2 where

$$F_T(x|\mu,\sigma_\theta^2)=\frac{\int_0^x e^{\sigma_\theta^{(-2)}\cos(t-\mu)dt}}{2\pi I_0\sigma_\theta^{-2}}, \quad (3)$$

and $I_0(x)=\sum_{m=0}^{\infty}1/(m!\Gamma(m+1))(x/2)^{2m}$ is a modified Bessel function of order 0.

Let us first denote the minimum angular distance between TD and ND ($|\theta_{ND}-\theta_{TD}|$) as $\theta_{\min}$, and the accuracy of this algorithm $(1-P_e)$ as r. Then, we can derive the accuracy of this technique from (2) as

$$r=F_T\left(\frac{\theta_{\min}}{2\sigma_\theta}\middle|0,\sigma_\theta^2\right). \quad (4)$$

Because $F_T(x|0,\sigma_\theta^2)$ is a non-decreasing function of x and a decreasing function of σ_θ^2, we achieve higher accuracy as the angular separation between TD and ND increases and/or the variance of magnetometer decreases. We corrobrotate the results using simulations later in Section 3.

2.3 AoA estimation-based device identification

The AoA-based algorithm assumes that the user device has multiple antennas and identifies the TD by estimating the incident angle of the TD's signal at the UD.

The UD broadcasts a request.

All NDs respond to the request by sending their IDs.

To estimate accurately, repeat the first and second step for T times.

Using multiple antennas, UD estimates the incident angles ($\hat{\phi}_D$) of the signals from each device D.

UD chooses the device which appears to be the closest to the heading angle of UD itself (90°) as the TD.

For AoA estimation, we leverage the fact that the signals from NDs at UD appear as plane waves, as they are relatively far apart from UD [6]. The steering vector $s(\phi)$ which represents the phase differences of a received signal at each antenna, has a one-to-one relationship with the direction of signal ϕ. If there are N antennas at UD and M incident signals, the covariance matrix Q of the received signal can be decomposed as $[Q_n Q_s]$ where Q_n is $N-M$ columns of eigenvectors corresponding to noise subspace, and Q_s is

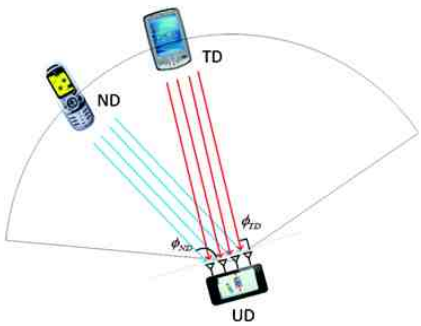

[Fig. 2] AoA-based D2D link association

M columns of eigenvectors corresponding to signal subspace. Here, because Q_n and $s(\phi)$ are orthogonal, we can identify the angles of arrival using the peaks of the following function $P_{MSIC}(\phi)$ [6],

$$P_{MUSIC}(\phi)=\frac{1}{\sum_{m=1}^{N-M}|s^H(\phi)q_m|^2}=\frac{1}{\|Q_n^H s(\phi)\|^2} \quad , (5)$$

Note that ϕ is equal to one of the angles of the incident signals, the denominator $\|Q_n^H s(\phi)\|$ becomes theoretically zero due to the orthogonality when the noise does not exist.

So far we have assumed the ideal behavior without considering any source of error. However, in practice, due to the effect of noise the denominator (5) cannot be zero. In addition, the correlation matrix of received signal R (in step 3) is unknown and must be estimated from the received data. This estimation requires averaging over several snapshots of data,

$$R=\frac{1}{T}\sum_{t=1}^{T}x_t x_t^H, \quad (6)$$

where x_t is the t-th data and T is the number of snapshots. If the received data is Gaussian, this estimate asymptotically converges to the true correlation matrix. T must be greater than $2N$ for the SNR to be within 3dB from the optimum [6].

If $|\hat{\phi}_{TD}-90^o|\le|\hat{\phi}_{ND}-90^o|$, UD erroneously selects ND as the target. The misidentification probability can be written as:

$$P_e=P[|\hat{\phi}_{TD}-90^o|\le|\hat{\phi}_{ND}-90^o|]. \quad (7)$$

Here, $\hat{\varphi}_{D_i}$ can be defined as follows:

$$\hat{\varphi}_{D_i}=\pi\cos(\hat{\phi}_{D_i}), \quad (8)$$

Because the expectations of estimated angle and variance are

$$E[\hat{\phi}_{D_i}]=\varphi_{D_i}, \quad (9)$$

$$\sigma_{D_i}^2=\frac{1}{2SNR_{D_i}T}\left[1+\frac{[(s(\phi)^H s(\phi))^{-1}]_{ii}}{SNR_{D_i}}\right]\frac{1}{h(\varphi_{D_i})}, \quad (10)$$

where SNR_{D_i} is the SNR of the signal from device D_i, $h(\phi)$ is a function of the incident angle, $s^H(\phi)Q_nQ_n^Hd(\phi)$, $d(\phi)$ is the first derivative of $s(\phi)$, $ds(\phi)/d\phi$ and $i=1,2$ for TD and ND, respectively [6].

Note the expected value of the estimated incident angle $\hat{\phi}_{TD}$ is 90° and that of $\hat{\varphi}_{TD}$ is 0°. Because $\hat{\phi}_{TD}$ and $\hat{\varphi}_{TD}$ follow the Gaussian distribution, $\hat{\phi}_{TD}$ is approximately Gaussian distributed near the expected value. Since the mismatching mostly occurs when ND is located near TD, we apply this approximation to ND as well as TD. Then, from (7), we have

$$P_e=P[|\hat{\phi}_{TD}-90^o|\le|\hat{\phi}_{ND}-90^o|]=P[|\hat{\varphi}_{TD}|\le|\hat{\varphi}_{ND}|]. \quad (11)$$

Using the expected values, variances and distributions of $\hat{\varphi}_{TD}$ and $\hat{\varphi}_{ND}$, we obtain the probability density functions of random variables $|\hat{\varphi}_{TD}|$ and $|\hat{\varphi}_{ND}|$ as follows:

$$f_{|\phi_{TD}|}^{MU}(x)=\frac{2}{\sqrt{2\pi\sigma_{TD}^2}}exp\left(-\frac{x^2}{2\sigma_{TD}^2}\right). \quad (12)$$

$$f_{|\phi_{ND}|}^{MU}(x)=\frac{2}{\sqrt{2\pi\sigma_{ND}^2}}\left[\exp\left(-\frac{(y-\mu_{ND})^2}{2\sigma_{ND}^2}\right)+\exp\left(\frac{(y+\mu_{ND})^2}{2\sigma_{ND}^2}\right)\right] \quad (13)$$

Hence, the mismatching probability is derived as

$$P_e = \int_0^{\infty}\int_0^{y} f^{MU}_{|\phi_{TD}|}(x) f^{MU}_{|\phi_{ND}|}(y)dxdy \qquad (14)$$
$$= \int_0^{\infty} 2erf\left(\frac{y}{\sigma_{TD}}\right) f^{MU}_{|\phi_{ND}|}(y)dy,$$

where the error function $erf(x) = 1/2\pi \int_0^x \exp(-x^2/2)dx$, $F^{MU}_{|\phi_{TD}|}$ is the cumulative density function of $|\hat{\phi}_{TD}|$, and $F^{MU}_{\phi_{TD}}$ is that of $\hat{\phi}_{TD}$. Further, we derive the CR variances as

$$var^{CR}_{D} = \left(\frac{1}{2\,TSNR_D}\right)\frac{1}{h(\varphi_D)} \qquad (15)$$

For a device D by the property that (10) converges to the CR variance as the number of antennas or SNR increase. Finally, from (15), we get the following mismatch probability:

$$P_e = \int_0^{\infty} 2erf\left(\frac{y}{\sqrt{var^{CR}_{TD}}}\right) f^{M}_{|\phi_{ND}|}(y)dy. \qquad (16)$$

3. Performance Analysis

We now present the performance of proposed GPS-based and AoA-based device identification algorithms. First, we evaluate the GPS-based scheme. We assume that UD has a single antenna, TD is located directly in front of the UD, and NDs are placed at other random locations. Here, we consider the distances from UD to TD and ND are exactly same. In other words, we do not consider the effect of received signal strength. Table 1 represents the minimum angular distances having the accurate identification probability greater than 0.95 or 0.99 in terms of the variance of the magnetometer in UD. The minimum angular distance means the smallest angular separation between TD and ND satisfying the algorithm's accuracy. From the table 1, we can observe the minimum angular distance becomes smaller as the variance of the magnetometer of UD decreases. This result is what we expected from (5).

[Table 1] The minimum angular distance satisfying the required system reliability

Minimum Angular Distance		
σ^2_θ	Accuracy	
	95%	99%
10	35.41	44.18
8	26.53	32.83
5	20.61	25.50
3	18.39	22.69

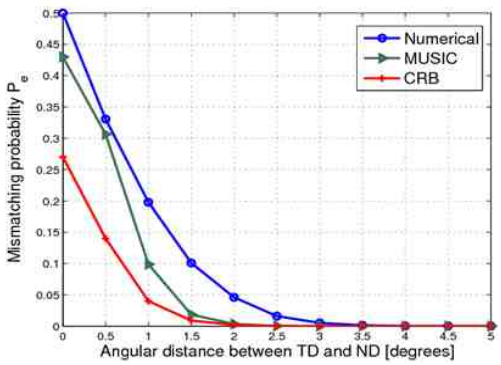

[Fig. 3] The mismatching probability according to the angular distance between TD and ND, when N=4, T=10, SNR=20 dB

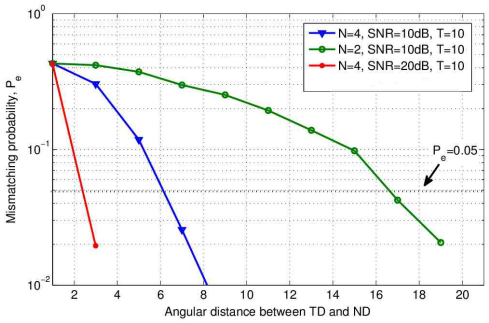

[Fig. 4] The mismatching probability according to the angular distance between TD and ND

Second, we evaluate the AoA estimation-based device identification technique. We compare the mismatching probabilities of (14) and (16) with that of numerical method as shown in Fig. 3. Note that it is well known the distribution of numerical estimation and that of the MUSIC estimator converge to the Gaussian distribution with CR variance when SNR goes high and the number of snapshot is enough [6]. Although we restrict the number of snapshot as 10 with 4 transmit antennas at moderate SNR, 20 dB, the result in Fig. 3 shows that mismatching does not occur if TD and ND are separated more than 3.5° for all three cases. Hence, the derived mismatching probabilities of (14) and (16) can be applied for analyzing the accuracy performance, instead of the numerical method. We use mismatching probabilities of the MUSIC estimator (14) for the analysis from now on.

Fig. 4 presents the mismatching probabilities with respect to the angular distances between TD and ND. We investigate the effect of the changes in SNR, the number of snapshot, and number of antenna to the mismatching probability. The numerical results corroborates (14) as the number of UD antennas increases or as the SNR increases, the mismatching probability decreases. For example, shows better performance than with same SNR and the number of snapshot (SNR=20dB and T=10). The mismatching probability is smaller when the SNR is stronger (20dB versus 10dB). In addition, the number of snapshot also affects the mismatching probability, when we reduce the number of snapshot to 1, the mismatching probability increases as shown in Fig. 4. With respect to the accuracy and the angular distance between TD and ND, the lower mismatching probability means the smaller dispersion between TD and ND for achieving the same target accuracy of the system. For example, TD and ND are required to be separated at least 3° when , T=10 and SNR=20dB (red line). However, separation of 6° is required when .

We have investigated the performance of both proposed techniques in terms of accuracy performance. Both techniques shows promising results in that the minimum angular distance between TD and ND is reasonable even in the face of noise. In addition, system requirements are realistic. Thus, we conclude that both techniques can be applied for establishing D2D communication.

4. Conclusion

In this work, two device identification techniques for user-friendly D2D communications have been proposed. First device identification technique uses the GPS and magnetometer, and the second one adopts super-resolution algorithm with multiple

antennas. We have analyzed the mismatching probabilities of both techniques. Also, we derive a minimum angular separation between adjacent devices to satisfy the required accuracy. The performance of the proposed techniques is presented using numerical evaluations.

Our work is the first work that utilizes the directional information for link association techniques, especially for D2D communication. We analyze performance of the proposed methods with basic assumptions. The performance comparison with practical system model remains as future work. We believe our user-friendly methods for point-and-link device identification can be used many applications to establish D2D communication.

Acknowledgement

This work has been supported by the National GNSS Research Center program of Defense Acquisition Program Administration and Agency for Defense Development

References

[1] Cisco Visual Networking Index: Forecast and Methodology, 2009-2014, 2010. http://www.cisco.com/en/US/solutions/collateral/ns341/ns525/ns537/ns705/ns827/white_paper_c11-481360_ns827_Networking_Solutions_White_Paper.html

[2] K.Doppler, M. Rinne, C, Wijting, C. Ribeiro, and K. Hugl, "Device-to-device communication as an underlay to LTE-advanced networks," *Communication Magazine, IEEE,* vol. 47, no. 12, pp. 42-49, 2009.

[3] M. S. Corson, R. Laroia, J. Li, V. Park, T. Richardson, and G. Tsirtsis, "Toward proximity-aware internetworking," *Wireless Communications, IEEE*, vol. 17, no. 6, pp. 26-33, 2010.

[4] B.-J. Kwak, S.-A. Kim, Y.-H. Kim, and N.-O. Song, "Random jitter beamforming for point-and-link communications," in *Statistical Signal Processing Workshop (SSP), IEEE,* pp.496-499, 2012.

[5] Fudge, Gerald L., and Darel A. Linebarger, "A calibrated generalized sidelobe canceller for wideband beamforming," *IEEE trans. on Signal Processing,* vol. 42, no. 10, pp. 2871-2875, 1994.

[6] N. A. P. Stoica, "MUSIC, maximal likelihood, and Cramer-Rao bound," *IEE trans. on Acoust., Speech, and Sig. Proc.*, vol. 37, no. 5, pp. 720-741, May 1989.

[7] R., Roy, R., T. Kailath, "ESPRIT-estimation of signal parameters via rotational invariance techniques," *IEEE Trans. on Acoust., Speech, and Sig. Proc.,* vol. 37, no. 7, pp. 984-995, 1989.

[8] Parkinson, Bradford W., and James J. Spilker, eds. *Global Positioning System: Theory and Applications*. Vol. 1. Aiaa, 1996.

[9] M. A. Stephens, "Use of the Von Mises distribution to analyse continuous propertions," *Biometrika,* vol. 69, no. 1, pp. 197-203, 1982.

Author Biography

Eun-hye Park [Member]

- Aug. 2011 : KAIST, Electrical engineering, BS
- Aug. 2013 : KAIST, Electrical engineering, MS
- Sep. 2013~current : KAIST, Electrical engineering, Ph. D. candidate

<Research Interests>
Device-to-device communication, Location based service application, Cognitive Radio

Kwang-Eog Lee [Member]

- Feb. 1988 : Kyungpook National University, Electronicsl engineering, BS
- Feb. 1990 : Kyungpook National University, Electronicsl engineering, MS
- Sep. 1990~current : Agency for Defence Development (ADD)

<Research Interests>
Cognitive radio, dynamic spectrum access in tactical satellite/ground communication

Joon-hyuk Kang [Member]

- Feb. 1991 : Seoul National University, Control and measurement engineering, BS
- Feb. 1993 : Seoul National University, Control and measurement engineering, MS
- Feb. 2002 : The University of Texas at Austin, Electrical & Computer engineering, Ph. D.
- Feb. 2002 - current : professor at KAIST, dept. of Electrical engineering

<Research Interests>
Massive MIMO, Cognitive Radio, Cooperative communications, Wireless localization